

Temporal Knowledge Graph Forecasting with Neural ODE

Zifeng Ding^{*3}, Zhen Han^{*1,2}, Yunpu Ma^{†*1}, Volker Tresp^{†1,2}

¹Institute of Informatics, LMU Munich ² Corporate Technology, Siemens AG

³Department of Electrical and Computer Engineering, Technical University of Munich

zhen.han@campus.lmu.de, zifeng.ding@tum.de

cognitive.yunpu@gmail.com, volker.tresp@siemens.com

ABSTRACT

Learning node representation on dynamically-evolving, multi-relational graph data has gained great research interest. However, most of the existing models for temporal knowledge graph forecasting use Recurrent Neural Network (RNN) with discrete depth to capture temporal information, while time is a continuous variable. Inspired by Neural Ordinary Differential Equation (NODE), we extend the idea of continuum-depth models to time-evolving multi-relational graph data, and propose a novel Temporal Knowledge Graph Forecasting model with NODE. Our model captures temporal information through NODE and structural information through a Graph Neural Network (GNN). Thus, our graph ODE model achieves a continuous model in time and efficiently learns node representation for future prediction. We evaluate our model on six temporal knowledge graph datasets by performing link forecasting. Experiment results show the superiority of our model.

1. INTRODUCTION

A Knowledge Graph (KG) is a graph structured knowledge base containing human knowledge and facts. It is widely used to study complex problems regarding human activities. A KG uses triplets (s, r, o) to represent the facts [29], where s, o, r means subject entity, object entity and the relation between them, respectively. However, if we want to model the reality, representing the facts in such triplets is not enough. The relation between two specific entities may change over time, which means the triplets may not be true forever. To represent the temporal events happening at a specific time, quadruples (s, r, o, t) are introduced by incorporating the event time t into the triplets from semantic KGs. A knowledge graph which uses the quadruples (s, r, o, t) to describe the events is called a temporal knowledge graph (tKG).

tKG reasoning has gained great research interest. Some works [30][9][12][14] focus on tKG completion, i.e. interpolated tKG reasoning, while other works [15][18][8] pay attention to future forecasting, i.e. extrapolated tKG reasoning. Given a sequence of observed events in a time period $t \in [t_1, t_T]$, for interpolated tKG reasoning, unseen events within this time period are to be predicted, however, for ex-

trapolated tKG reasoning, unseen events which occur after t_T are to be predicted. In our work, we focus on extrapolated tKG reasoning by designing a model for future link prediction.

Modeling tKG dynamics is critical in solving tKG reasoning problems. We characterize tKG dynamics as a changing state by learning time-aware entity representations and relation representations. Inspired by neural ordinary differential equations (NODEs) [5], we extend the idea of continuum-depth models to encoding tKG dynamics. NODE-based models use ordinary differential equations (ODEs) to model the continuous dynamics of a dynamic system. To apply NODEs to tKG reasoning, we employ a NODE coupled with graph neural network (GNN) [34] layers. GNN layers are used to capture the structural information of graph data, while the NODE works as a tool to learn the evolution of the tKG dynamics over time, including the dynamic representation of entities and relations. We integrate the tKG state over time, and output the time-aware dynamic representation directly from taking the integration result at any time. During the integration in NODE, the graph state goes through a continuum-depth of GNN layers. The exact depth of the GNN-based module is controlled by the length of integration, i.e. the length of time. Unlike many existing tKG reasoning models which learn tKG dynamics by employing recurrent model structure with discrete depth, our model takes advantage of NODE to interpret the time duration between the timestamps in tKGs as a continuum depth in the network structure, making it possible to learn a continuous tKG dynamics over time.

Besides, to better learn tKG dynamics, we propose a novel stochastic jump method to model the influence of the stochastic events occurring over time. In various real-world situations[11][16][23], the system dynamics evolves continuously until some stochastic events occur to interrupt it. By analyzing the appearance and the disappearance of triplets (s, r, o) over time, we formally define a new kind of stochastic jump events, acting as the stochastic events occurring in the context of tKG databases, and use a GNN-based stochastic jump layer to capture their influence.

In this work, we propose a model to perform tKG link Forecasting with NODE. The main contributions of our work are summarized as follows:

- We propose a graph reasoning model for extrapolated link prediction on temporal knowledge graphs (tKGs). We study a new approach to derive time-aware dynamic representations for graph data based on neural

^{*}Equal contribution.

[†]Corresponding authors.

ordinary differential equations (NODEs). The NODE enables our model to learn continuous representations of entities and relations over time, while previous models can only learn discrete graph representations specified at some timestamps. Our model is the first model that adapts NODEs to learning the tKG dynamics.

- We define a new kind of stochastic jump events for tKG databases and propose a novel stochastic jump method to learning their influence. The method does not require additional data and can effectively improve our model performance.
- We propose two new tasks, namely inductive link prediction and long horizontal link forecasting, for tKG representation learning models. They evaluate a model’s potential by testing the model performance on previously unseen entities and predicting the links happening in the farther future, respectively.
- Our model can achieve state-of-the-art performance on extrapolated link prediction on tKGs.

2. BACKGROUND AND RELATED WORK

2.1 Graph Convolutional Networks

Graph neural networks (GNNs) have shown strong performance in learning graph data. A large number of GNNs are designed based on the idea of generalizing convolution in CNN to graph learning scenarios. Some works use spectral method, e.g. [20][7], while other works use spatial method, e.g. [26][10]. The definition of Kipf et al. [20] has become the most popular among all the works regarding Graph Convolutional Network (GCN), and most further GCN variants are developed on top of it. In [33], a GCN variant named Composition-based Multi-relational Graph Convolutional Network (COMP GCN) is proposed to leverage a variety of entity-relation composition operations from Knowledge Graph Embedding (KGE) techniques. It is compatible with KGs and it also generalizes several of the existing multi-relational GCN models. We derive our GNN module on top of [33], and generalize it into the context of tKG, aiming to learn tKG dynamics for extrapolated link prediction.

2.2 Neural Ordinary Differential Equations

Neural Ordinary Differential Equation (NODE) [5] is a continuous deep neural network model. It represents the derivative of the hidden state with a neural network:

$$\frac{d\mathbf{z}(t)}{dt} = f(\mathbf{z}(t), t, \theta) \quad (1)$$

where $\mathbf{z}(t)$ denotes the hidden state of the whole system at time point t , and f denotes a function defined by a neural network to describe the derivative of the hidden state w.r.t. time. θ represents the parameters in the neural network which defines f .

The output of a NODE system is calculated by using an ODE solver coupled with an initial value problem:

$$\mathbf{z}(t_1) = \mathbf{z}(t_0) + \int_{t_0}^{t_1} f(\mathbf{z}(t), t, \theta) dt \quad (2)$$

Here, t_0 is the initial time point and t_1 is the output time point. $\mathbf{z}(t_1)$ and $\mathbf{z}(t_0)$ represent the hidden state at t_0 and t_1 , respectively. Thus, a NODE can output the hidden state of a

dynamic system at any time point and deal with continuous data, which is extremely useful in modeling continuous and dynamic systems.

Moreover, to reduce the memory cost in the backpropagation, Chen et al. [5] introduced the adjoint sensitivity method [28] into NODEs. An adjoint $\mathbf{a}(t) = \frac{\partial \mathcal{L}}{\partial \mathbf{z}(t)}$, where \mathcal{L} is loss. The gradient of loss \mathcal{L} w.r.t. network parameters θ can be directly computed by using the adjoint and an ODE solver:

$$\frac{d\mathcal{L}}{d\theta} = - \int_{t_1}^{t_0} \mathbf{a}(t)^T \frac{\partial f(\mathbf{z}(t), t, \theta)}{\partial \theta} dt \quad (3)$$

which means these gradients do not need to be stored in the process of backpropagation, thus reducing memory cost.

2.2.1 Temporal Knowledge Graph Reasoning

There have been some recent works related to tKG reasoning. [30] and [15] take advantage of temporal point processes to model the tKG event sequences over time. For a tKG quadruple (s, r, o, t) , [21] and [9] incorporate time information t into the existing embedding techniques, e.g. TransE [3], by designing time aware embedding techniques. [30][18][8][14] learn tKG dynamics as a graph state which evolves over time for tKG reasoning. Most previous works are designed for interpolated tKG reasoning, while only a few models, e.g. [30][18][8], are designed for future forecasting.

3. OUR MODEL

We present our model in this section. Our model is designed to model dynamically-evolving, multi-relational, large-scale graph data by jointly learning entity representations and relation representations. It consists of a NODE-based encoder and a KG-oriented decoder. The application of the NODE enables our model to learn a continuous graph representation. To capture structural graph information, we employ a modified version derived by two GNN modules, Graph Convolutional Network (GCN) [20] and Composition-based Multi-relational Graph Convolutional Network (COMP GCN) [33], inside NODE. For the KG-oriented decoder, we use two decoders for comparison, i.e. Distmult [35] and TuckER [1].

To show the strength of our model, we perform extrapolated link prediction on tKGs. Details of the experiments will be presented in section 4. In the following part of this section, we will first explain our task and then provide the details of our model.

3.1 Task Formulation

In our work, we focus on tKGs represented by graph slices over time. A tKG can be described as $\mathbb{G} = \{\mathcal{G}(1), \dots, \mathcal{G}(T)\}$. Here, T denotes the number of timestamps, and $\mathcal{G}(t) = (\mathcal{V}, \mathcal{E}(t))$ is the graph snapshot at the t . \mathcal{V} denotes all the vertices, i.e. tKG entities, in \mathbb{G} , and $\mathcal{E}(t) = \{(s_i, r_i, o_i, t)\}_{i=1}^{N_t}$ denotes all the events occurring at t .

Formally, we describe our task in the following way. Consider a tKG $\mathbb{G} = \{\mathcal{G}(1), \dots, \mathcal{G}(T)\}$. To perform link prediction, we aim to predict the missing object entity for every object prediction query $(s, r, ?, t)$. All the prediction queries are derived by removing the object from a tKG event. In our work, we augment every quadruple (s, r, o, t) with another quadruple (o, r^{-1}, s, t) where r^{-1} means the reciprocal relation of r . Therefore, both object and subject prediction are

considered without a loss of generality. To do this task, we first compute the scores of the triplets (s, r, v) by replacing v in the query with every entity $v \in \mathcal{V}$. Then we sort the scores in descending order and find out the rank of the score related to the correct missing object. The higher the rank is, the better the model performs.

We pay attention to the extrapolated setting of tKG reasoning and perform future link prediction. For example, given the observed tKG snapshots $\mathbb{G} = \{\mathcal{G}(t_0), \dots, \mathcal{G}(t_1)\}$, we aim to predict the missing objects in the prediction queries corresponding to the events occurring after t_1 . From section 3.2 to section 3.5, we explain how we design our model and how it deals with this task.

3.2 Relational Graph Aggregator

GNN-based models have shown great effect on capturing structural information of graph data. To deal with the relations existing in tKGs, we use a relational aggregator derived on top of the model proposed by [33]. At t , for every object entity $o \in \mathcal{V}$, with $\mathcal{N}(o) = \{(s, r) | (s, r, o, t) \in \mathcal{E}(t)\}$, o 's entity representation evolves as follows:

$$\mathbf{h}_o^{l+1} = \sigma \left(\frac{1}{|\mathcal{N}(o)|} \sum_{(s,r) \in \mathcal{N}(o)} \mathbf{W}_{\text{ent}}^l \phi(\mathbf{h}_s^l, \mathbf{h}_r^l) \right) \quad (4)$$

$\mathbf{W}_{\text{ent}}^l$ is a trainable weight matrix on the l^{th} layer and ϕ denotes a composition-based operator inspired by [33]. We take $\phi(\mathbf{h}_s, \mathbf{h}_r) = \mathbf{h}_s * \mathbf{h}_r$. Additionally, we employ another weight matrix for learning relation representation:

$$\mathbf{h}_r^{l+1} = \mathbf{W}_{\text{rel}}^l \mathbf{h}_r^l \quad (5)$$

From the view of the whole graph, we can represent our relational graph aggregator as follows:

$$\mathbf{H}^{l+1} = f(\mathbf{H}^l, \mathbf{W}_{\text{ent}}^l, \mathbf{W}_{\text{rel}}^l, \mathcal{G}_t) \quad (6)$$

where f denotes the neural network layer specified by the relational graph aggregator. $\mathbf{H} \in \mathbb{R}^{(|\mathcal{V}|+N_r) \times d}$ is the hidden state of the graph. N_r is the number of relations, and each row of H represents the entity representation of an entity or the relation representation of a relation. By using this aggregator, we can effectively capture the structural information of knowledge graphs.

3.3 Learning tKGs with NODE

To incorporate time information, we use a NODE coupled with our relational graph aggregator. In this section, we present how we capture temporal dependencies on tKGs with NODE.

3.3.1 Graph Convolutional NODE

Given a tKG $\mathbb{G} = \{\mathcal{G}(1), \dots, \mathcal{G}(T)\}$, we can use our relational graph aggregator to learn its entity representation and relation representation. Similar to Eq.(1), we can combine the aggregator with a NODE:

$$\frac{d\mathbf{H}(t)}{dt} = F(\mathbf{H}(t), t, \Theta, \mathcal{G}(t)) \quad (7)$$

Here, $\mathbf{H}(t) \in \mathbb{R}^{(|\mathcal{V}|+N_r) \times d}$ denotes the hidden state of the graph at t . F denotes a neural network which consists of stacked layers (or a single layer) of the relational graph aggregator, and Θ denotes all the parameters of F . And the

output of the system at $t+1$ can also be formulated according to Eq.(2):

$$\mathbf{H}(t+1) = \mathbf{H}(t) + \int_t^{t+1} F(\mathbf{H}(t), t, \Theta, \mathcal{G}(t)) dt \quad (8)$$

In this way, we manage to use the NODE to learn the dynamics of tKGs.

3.3.2 Residual Layer

To improve the performance of our model, we change the relational graph aggregation layer stated in Eq.(6) into a residual layer:

$$\mathbf{H}^{l+1} = \mathbf{H}^l + \delta f(\mathbf{H}^l, \mathbf{W}_{\text{ent}}^l, \mathbf{W}_{\text{rel}}^l, \mathcal{G}) \quad (9)$$

where δ is a trainable parameter which is used to control how much residual information we want to learn. We can also change Eq.(7) and Eq.(8) into:

$$\begin{cases} \frac{d\mathbf{H}(t)}{dt} = F_{\text{agg}}(\mathbf{H}(t), t, \Theta_{\text{agg}}, \mathcal{G}(t)) \\ \mathbf{H}(t+1) = \mathbf{H}(t) + \int_t^{t+1} F_{\text{agg}}(\mathbf{H}(t), t, \Theta_{\text{agg}}, \mathcal{G}(t)) dt \end{cases} \quad (10)$$

where F_{agg} , illustrated in Figure 1 (a), now represents a neural network which consists of several stacked (or a single) residual aggregation layers, and $\Theta_{\text{agg}} = \{\Theta, \delta\}$ denotes all the parameters in F_{agg} .

3.4 Stochastic Jump Method

The dynamics of a system can be influenced by the occurrence of stochastic events. In previous works [17][11][16][23], stochastic events represent the stochastically incoming data over time which incur changes in the system dynamics. In our work, we define a new kind of stochastic events in tKGs named stochastic jump events, and use a GNN-based stochastic jump layer to capture the influence. By including the influence of stochastic jump events, we can effectively enhance our model performance.

3.4.1 Motivation

In tKGs, KG facts are not always valid or invalid. Assume we have a KG fact, described as a triplet (s, r, o) , which is valid at t . However, it is not valid at $t+1$, which means it disappears over time from t to $t+1$. Similarly, a KG fact that is invalid at t may be valid at $t+1$, which can be taken as the appearance of this fact over time from t to $t+1$. The change of tKG events over time can therefore be interpreted as the appearance and the disappearance of KG facts, and this change contains implicit information which is helpful in graph representation learning. For example, we have a KG fact $(x, \text{Reject economic cooperation}, y)$, where x, y denote two countries. It is invalid at t , but it becomes valid at $t+1$. Besides, we have another KG fact $(x, \text{Threaten with sanctions}, y)$ which is valid at $t+2$. Intuitively, the appearance of $(x, \text{Reject economic cooperation}, y)$ implies the existence of $(x, \text{Threaten with sanctions}, y)$ after $t+1$, thus providing implicit information for link forecasting. We define the change of tKG events over time as stochastic jump events and design a method to capture the information brought by them. By applying this method, we can better model the changes in tKG dynamics between timestamps and better learn entity and relation representations.

3.4.2 Stochastic Jump Events for tKGs

The formal derivation of the stochastic jump event which occurs at t is defined as follows. Assume we have two tKG snapshots $\mathcal{G}^{(t)}$ and $\mathcal{G}^{(t+1)}$, we construct the following jump tensor to denote the changes in tKG events from t to $t+1$:

$$\mathbf{T}^\Delta(t) = \mathbf{T}(t+1) - \mathbf{T}(t) \quad (11)$$

$\mathbf{T}(t) \in \mathbb{R}^{|\mathcal{V}| \times N_r \times |\mathcal{V}|}$ is a tensor containing the information of the existence of all KG triplets (s, r, o) at t . If (s, r, o) exists at t , which means there exists a tKG event (s, r, o, t) , $\mathbf{T}(t)_{sro} = 1$, otherwise, $\mathbf{T}(t)_{sro} = 0$. Intuitively, \mathbf{T}^Δ contains the information of the appearance and the disappearance of the triplets among tKG entities and relations. If $\mathbf{T}^\Delta(t)_{sro} = -1$, that means there exists a triplet (s, r, o) at t , but it disappears at $t+1$. Similarly, $\mathbf{T}^\Delta(t)_{sro} = 1$ means that there appears a triplet (s, r, o) at $t+1$ while there is no such triplet at t . For the other elements in $\mathbf{T}(t)$, their values are equal to 0, indicating the existence, or inexistence, of the corresponding triplets remains unchanged. We take \mathbf{T}^Δ over time to represent the stochastic jump events for tKGs, and we use a GNN-based module to extract the information provided by them.

$$\begin{cases} \Delta \mathbf{h}_o^{l+1} = \sigma \left(\frac{1}{|\mathcal{N}_{T^\Delta}(o)|} \sum_{(s,r) \in \mathcal{N}_{T^\Delta}(o)} \mathbf{W}_{\text{jump_ent}}^l (\mathbf{T}_{sro}^\Delta \phi(\mathbf{h}_s^l, \mathbf{h}_r^l)) \right) \\ \Delta \mathbf{h}_r^{l+1} = \mathbf{W}_{\text{jump_rel}}^l \mathbf{h}_r^l \end{cases} \quad (12)$$

Here, $\mathcal{N}_{T^\Delta}(o) = \{(s, r) | \mathbf{T}_{sro}^\Delta \neq 0\}$, $\mathbf{W}_{\text{jump_ent}}$ and $\mathbf{W}_{\text{jump_rel}}$ are two diagonal trainable weights for the stochastic jump layer. $\phi(\mathbf{h}_s, \mathbf{h}_r) = \mathbf{h}_s * \mathbf{h}_r$ is defined as same in the graph aggregation layer. By employing this stochastic jump layer, we enable our model to preserve the graph structure as it learns from the stochastic jump events. The output of the jump module is then defined as:

$$\mathbf{H} = \mathbf{H}_{\text{agg}} + w f_{\text{jump}}(\mathbf{H}, \mathbf{W}_{\text{jump_ent}}, \mathbf{W}_{\text{jump_rel}}, \mathbf{T}^\Delta) \quad (13)$$

\mathbf{H}_{agg} is the output of the stacked layers of relational graph aggregator and f_{jump} is the stochastic jump layer. w is a hyperparameter with a fixed value, acting as the coefficient deciding how much the model learns from stochastic jump events. Notice that the stochastic jump layer takes the graph hidden state before graph aggregators as its input. By combining our relational graph aggregation layers and the stochastic jump method, we get our final network F_{model} applied in the NODE. The network structure is described in Figure 1 (b).

3.5 Learning and Inference with Our Model

Our model is an autoregressive model. It specifies the entity representation at a specific time point t by utilizing the graph information before t . To perform the link prediction task, our model takes three steps. First, our model computes the graph representation at the query timestamp. Then our model uses KG decoders to compute the scores of all the (s, r, o) triplets of interest. Finally, our model ranks the scores of the potential missing entities and does the prediction.

We will present the parameter learning and the extrapolated link prediction procedure in this section.

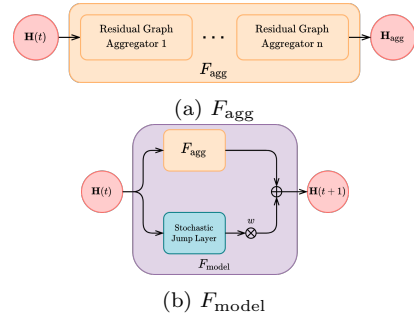


Figure 1: The structure of the neural networks inside NODE. $\mathbf{H}(t)$ and $\mathbf{H}(t+1)$ denote the graph hidden state at t and $t+1$, respectively. \mathbf{H}_{agg} denotes the output of the stacked graph aggregation layers. (a) The structure of F_{agg} : stacked residual relational graph aggregation layers (orange blocks). n is the number of layers in F_{agg} . The orange shaded area represents F_{agg} . (b) The complete structure of the neural network in our model: besides F_{agg} , a jump stochastic layer (cyan block) is employed to learn a shift in graph hidden representation. The purple shaded area represents F_{model} .

3.5.1 Temporal Graph Representation Inference

Assume we want to perform link prediction at $t+1$. To get the graph hidden state at $t+1$, we first let the graph hidden state at $t-k$, $\mathbf{H}(t-k)$, equal the global graph embedding $\mathbf{H}_{\text{global}} \in \mathbb{R}^{(|\mathcal{V}|+N_r) \times d}$. Here, $\mathbf{H}_{\text{global}}$ is a trainable parameter which acts as a universal input at timestamp $t-k$ for link prediction at any $t+1$. We take $\mathbf{H}(t-k) = \mathbf{H}_{\text{global}}$ as the NODE input at $t-k$, and integrate it with an ODE solver $\text{ODESolve}(\mathbf{H}(t-k), F_{\text{model}}, t-k, t-k+1, \Theta_{\text{model}})$ over time. We use $\mathcal{G}(t-k), \dots, \mathcal{G}(t)$ to specify the graphs in the relational graph aggregation layers in F_{model} from $t-k$ to t . As the hidden state evolves with time, it learns from different graph snapshots corresponding to the different time points. The whole process is described in Figure 2 and Algorithm 1 (Appendix A). In Figure 2, `set_graph` and `set_jump` stand for two functions used to feed graph snapshots \mathcal{G} and jump tensors \mathbf{T}^Δ into neural network F_{model} . They are called at every timestamp before integration. The output hidden state $\mathbf{H}(t+1)$ serves as the temporal graph representation at $t+1$.

3.5.2 Score Function

With the temporal graph representation at the prediction timestamp, we can compute the scores of every (s, r, o) triplets. In our work, we take advantage of two popular knowledge graph static models, i.e. Distmult [35] and TuckER [1]. Given a triplet (s, r, o) , its score is computed as shown in Table 1. The entity representation of s , o , and the relation representation of r are used for score computation, and they are learned together with other parameters by minimizing the loss function.

3.5.3 Parameter Learning and Model Training

For parameter learning, we employ the following loss function:

Table 1: Score Functions. $\mathbf{h}_s, \mathbf{h}_r, \mathbf{h}_o$ denote the entity representation of the subject entity s , object entity o , and the relation representation of the relation r , respectively. d_e is the dimension of each entity’s representation. $\mathcal{W} \in \mathbb{R}^{d_e \times d_r \times d_e}$ is the core tensor specified in [1], where d_r is the dimension of each relation’s representation. As defined in [31], $\times_1, \times_2, \times_3$ are three operators indicating tensor product in three different modes.

Method	Score Function
Distmult [35]	$\langle \mathbf{h}_s, \mathbf{h}_r, \mathbf{h}_o \rangle$ $\mathbf{h}_s, \mathbf{h}_r, \mathbf{h}_o \in \mathbb{R}^{d_e}$
TuckER [1]	$\mathcal{W} \times_1 \mathbf{h}_s \times_2 \mathbf{h}_r \times_3 \mathbf{h}_o$ $\mathbf{h}_s, \mathbf{h}_r, \mathbf{h}_o \in \mathbb{R}^{d_e}$

$$\mathcal{L} = \sum_t \sum_{(s,r,o,t) \in \mathcal{G}(t)} -\log \left(\frac{\exp(\text{score}(s,r,o))}{\sum_v \exp(\text{score}(s,r,v))} \right) \quad (14)$$

where $v \in \mathcal{V}$ represents an object candidate, and score is the score function used to compute the score of a triplet. In Eq.(14), we use the scores of the triplets together with the softmax function to compute the probability of an entity being the ground-truth object in each prediction query. Minimizing \mathcal{L} is as same as maximizing the probability of selecting the ground-truth entities.

During training, adaptive ODE solvers may incur huge time consumption in our work. To keep the training time tractable, we use fix grid ODE solvers coupled with the Interpolated Adjoint Method (IAM) proposed by [6]. IAM uses Barycentric Lagrange interpolation (BLI) [2] on a Chebyshev grid [32] to approximate the solution of the hidden state $z(t)$ in the reverse-mode of NODE. During backpropagation, we do not need to solve the following ODE:

$$\begin{cases} \frac{dz(t)}{dt} = f(\mathbf{z}(t), t, \theta), t \in [t_1, t_0] \\ \mathbf{z}(t_1) = \mathbf{z}_1 \end{cases} \quad (15)$$

because the value of $z(t)$ at any $t \in [t_1, t_0]$ can be approximated by the value of Chebyshev nodes which are saved before in the forward pass. IAM can lower the time cost in backpropagation and maintain good learning accuracy.

4. EXPERIMENTS

4.1 Experimental Setup

We evaluate our model by performing future link prediction on six tKG datasets. We compare our model’s performance with several existing methods and validate its potential with inductive link prediction and long horizontal link forecasting. Besides, an ablation study is conducted to show the superiority of our stochastic jump method.

4.1.1 Datasets

Six public tKG datasets are used for evaluation: 1) ICEWS14 [30] 2) ICEWS18 [4] 3) ICEWS05-15 [9] 4) GDELT [22] 5) WIKI [21] 6) YAGO [24].

Integrated Crisis Early Warning System (ICEWS) [4] is a dataset containing political events over time. We use three ICEWS datasets, namely ICEWS14, ICEWS18, and ICEWS05-15, for model evaluation. ICEWS14 contains all the events occurring in 2014, while ICEWS18 contains all the events

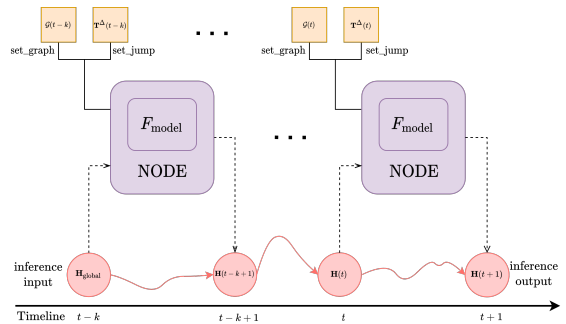


Figure 2: Illustration of the temporal graph representation inference procedure. The shaded purple area represents the whole model of our model. It is a Neural ODE equipped with GNN-based module F_{model} . Dashed arrows denote the input and the output path of the graph hidden state. Red solid arrows indicate the continuous hidden state flows learned by our model. Black solid lines represent that our model calls the function `set_graph` and `set_jump`. The corresponding graph snapshots \mathcal{G} and jump tensors \mathbf{T}^Δ are input into F_{model} for learning temporal graph information.

from January 1, 2018, to October 31, 2018. ICEWS05-15 is a long-term dataset that contains the events between 2005 to 2015. Global Database of Events, Language, and Tone (GDELT) [22] is a database recording all the events driving our global society every second of every day. We also use a subset of the complete database. The GDELT dataset used in our work contains all the data from January 1, 2018, to January 31, 2018. WIKI and YAGO are two datasets extracted from Wikipedia and the English WordNet dataset [25], respectively. We use the preprocessed version proposed in [18]. We follow the dataset split strategy in [18]. For every dataset except ICEWS14, we split it by timestamps into three parts, i.e. 80% – 10% – 10% (training-validation-test). For ICEWS14, we follow the split from [30], i.e. 50% – 50% (training-test). The detailed statistics of the datasets are presented in Appendix B.1.

4.1.2 Implementation Details

We train our model with the following setting. We set the length of input graph history to 4, and the embedding dimension of both entity and relation to 300. We use Adam optimizer [19] and set the learning rate to 0.001. To improve the precision in NODE training, we normalize the range of timestamps from 0 to 0.01. This step restricts the length of ODE integration, preventing the high error induced by ODE solvers. We use a fixed-grid ODE solver, Fourth Order Runge-Kutta, as the ODE solver, and implement the Interpolated Adjoint Method [6] with 3 Chebyshev nodes to keep training time tractable and maintain high precision at the same time. According to different datasets, we choose different values for the jump coefficient w . Our model is implemented with PyTorch [27] and all the experiments are run on GeForce RTX 2080 Ti.

4.1.3 Evaluation Metrics

We use two metrics to evaluate the model performance on extrapolated link prediction, namely Mean Reciprocal Rank (MRR) and Hits@k. MRR is the mean of the reciprocal values of the actual missing entities’ ranks for all the queries,

while Hits@k denotes the proportion of the actual missing entities which are ranked in the top k.

We also report the results in three settings, namely raw, time-unaware filtered, and time-aware filtered. For time-unaware filtered results, we follow the filtered setting proposed by [3], by removing from the list of corrupted triplets all the triplets that appear either in the training, validation, or test set except the test triplet of interest. Time-unaware filtered results are over-optimistic in many cases, while fairer results can be produced in the time-aware filtered setting. For time-aware filtered results, we follow the setting proposed by [15], by only removing from the list of corrupted triplets all the triplets that appear at the same timestamp of the test triplet of interest. We explain the difference between time-unaware and time-aware filtered results with the example stated in Appendix B.2. We report the raw results in Appendix B.4. By reporting the results in all three settings, we achieve a fair evaluation.

4.1.4 Baseline Methods

We compare our model performance with several existing baseline models. Both static methods and temporal methods are considered. We take several knowledge graph models as static KG reasoning baselines, including Distmult [35], TuckER [1] and COMPGCN [33]. We remove the timestamps in the quadruples for static methods, and only use the unique triplets (s, r, o) for training, validation, and test. In this case, the tKG collapses into a cumulative knowledge graph. Since we abandon the timestamps for static KG reasoning models, we can only report the model performance in the raw setting and in the time-unaware filtered setting. For tKG reasoning baselines, we report the performance of TTransE [21], TA-Distmult [9] and RE-Net [18]. Detailed experimental settings of baselines are presented in Appendix B.3.

4.2 Experiment Results and Ablation Study

We run all the baselines and our our model model five times and obtain the averaged results of all three settings, i.e. raw, time-aware filtered, and time-unaware filtered. On account of the lack of time information in static KG reasoning baselines, we can only compare the static baselines with our model in raw and time-unaware filtered settings.

4.2.1 Time aware ltered Results

The time-aware filtered results are presented in Table 2. As explained in section 4.1.3, we take the time-aware filtered setting as the fairest evaluation setting. Results demonstrate that our model outperforms all the models on every dataset. In this setting, Our model achieves much stronger results when it is coupled with Distmult on WIKI and YAGO, while it is works better with TuckER on every ICEWS dataset and GDEL T.

4.2.2 Time unaware Filtered Results

In Table 3, the time-unaware filtered results of all the models are presented. All the static KG reasoning baselines underperform compared with our model. This implies the importance of utilizing temporal information in tKG datasets. The comparison between Distmult and our model plus Distmult shows the superiority of our NODE-based encoder. This can also be observed with the comparison between TuckER and our model plus TuckER. Our model achieves

much better results than COMPGCN, indicating the strength of our method in incorporating temporal factors into tKG representation learning.

Similarly, our model outperforms all the tKG reasoning baselines as well. Different from TTransE and TA-Distmult, RE-Net uses a recurrent event encoder to capture temporal information, which shows a great effect on model performance. Our model also implements a NODE-based encoder in the recurrent style to learn temporal factors and it achieves even better results than RE-NET.

We can also observe that TTransE and TA-Distmult are beaten by static baseline methods on several datasets. The reason for this result is that TTransE and TA-Distmult are initially designed for interpolated graph completion. They can not reach the same performance on future link prediction because they are not allowed to use the graph information after the prediction timestamp in the extrapolated setting. Static baseline models are trained and tested on a static, cumulative knowledge graph, thus not considering timestamps in the extrapolated link prediction task. Different settings for static and temporal methods lead to this result.

4.2.3 Inductive Prediction Analysis

As reported in [13], in many real-world applications, new graph nodes emerge as time evolves, e.g. posts on Reddit. It is likely that the model deals with newly appeared nodes that are unseen in the training set. A superior model requires a strong generalization power to prove that it is capable of achieving good performance not only on the observed data, but also on the unseen data. We, therefore, propose a new task, namely inductive link prediction, to validate the model potential in predicting the links regarding previously unseen *entities* in the test set.

A test quadruple is selected for the inductive prediction, if either its subject or its object, or both of them act as unseen entities in the training set:

$$\{(s_{\text{induct}}, r, o, t)\} \cup \{(s, r, o_{\text{induct}}, t)\} \cup \{(s_{\text{induct}}, r, o_{\text{induct}}, t)\}$$

$s_{\text{induct}}, o_{\text{induct}}$ denote the unseen subjects and objects. An example of an inductive test quadruple is discussed in Appendix B.5. We then perform the extrapolated link prediction on these inductive prediction quadruples and the results are shown in Table 4. We compare our model with RE-NET, our strongest baseline, on ICEWS05-15. We also report the results achieved by our model without the stochastic jump method to show the performance boost brought by it.

As shown in Table 4, our model coupled with TuckER achieves the best results for all metrics in all settings. Regardless of which KG decoder is employed, our model can beat RE-Net, showing the strength of our model in inductive link prediction. The results achieved by our complete models are much better than their variants without the stochastic jump method, which proves that our proposed stochastic jump method plays an important role in inductive link prediction.

4.2.4 Long Horizontal Link Forecasting

In the regular extrapolated link prediction task, given the graph information in a specific time window, the links at the next upcoming timestamp are to be predicted. For example, given a sequence of graph snapshots $\mathbb{G} = \{\mathcal{G}(t-k), \dots, \mathcal{G}(t)\}$, whose length is k , the test quadruples happening at $t+1$ are to be predicted. However, in some contexts, the graph infor-

Datasets	ICEWS14 - dep filtered				ICEWS18 - dep filtered				ICEWS05-15 - dep filtered				GDELT - dep filtered				WIKI - dep filtered				YAGO - dep filtered			
Model	MRR	Hits@1	Hits@3	Hits@10	MRR	Hits@1	Hits@3	Hits@10	MRR	Hits@1	Hits@3	Hits@10	MRR	Hits@1	Hits@3	Hits@10	MRR	Hits@1	Hits@3	Hits@10	MRR	Hits@1	Hits@3	Hits@10
TTransE	6.89	1.36	6.60	18.18	8.08	1.84	8.25	21.29	15.52	4.70	19.20	38.27	5.50	0.49	4.99	15.18	29.27	21.67	34.43	42.39	31.19	18.12	40.91	51.21
TA-DistMult	10.34	4.72	10.54	21.48	11.38	5.58	12.04	22.82	24.39	14.77	27.80	44.22	11.17	5.09	11.58	22.65	44.53	39.92	48.73	51.71	54.92	48.15	59.61	66.71
RE-Net	25.66	16.69	28.35	43.62	27.90	18.45	31.37	46.37	40.23	30.30	44.83	59.59	19.58	12.45	20.90	33.44	49.66	46.88	51.19	53.48	58.02	53.06	61.08	66.29
Our encoder + TuckER	26.23	17.28	29.06	44.08	28.68	19.35	32.17	47.04	41.36	31.16	46.43	61.14	19.66	12.50	20.93	33.55	50.43	48.52	51.47	53.58	57.83	53.05	60.78	65.85
Our encoder + Distmult	24.69	16.30	27.17	41.52	26.75	17.92	30.08	44.09	39.98	30.37	44.72	58.57	19.17	12.15	20.35	32.82	51.15	49.66	52.16	53.35	62.70	59.18	65.31	67.90

Table 2: Extrapolated link prediction results on six datasets. Evaluation metrics are time-aware filtered MRR (%) and Hits@1/3/10 (%). The best results are marked in bold.

Datasets	ICEWS14 - indep filtered				ICEWS18 - indep filtered				ICEWS05-15 - indep filtered				GDELT - indep filtered				WIKI - indep filtered				YAGO - indep filtered			
Model	MRR	Hits@1	Hits@3	Hits@10	MRR	Hits@1	Hits@3	Hits@10	MRR	Hits@1	Hits@3	Hits@10	MRR	Hits@1	Hits@3	Hits@10	MRR	Hits@1	Hits@3	Hits@10	MRR	Hits@1	Hits@3	Hits@10
Distmult	20.07	14.49	21.34	30.31	29.01	23.22	31.15	40.01	35.09	29.02	37.24	46.30	26.95	19.60	28.36	39.77	26.26	25.70	26.45	27.17	54.69	53.82	54.67	56.24
TuckER	27.07	20.26	29.36	39.18	35.91	28.56	38.97	48.80	42.46	36.53	44.67	53.04	24.69	14.72	29.32	41.81	26.53	26.05	26.61	27.21	55.23	54.12	55.05	57.11
COMPGCN	22.03	14.81	24.11	35.97	30.36	22.74	33.09	45.10	36.96	29.50	39.86	51.35	26.19	18.13	29.01	40.99	27.13	26.16	27.16	28.12	55.77	54.09	55.52	58.76
TTransE	10.10	2.66	11.44	25.31	10.52	3.01	11.98	26.16	20.85	6.92	29.06	46.49	9.38	0.89	11.60	25.79	31.94	24.82	36.91	43.55	33.73	20.99	43.51	52.61
TA-DistMult	18.74	11.97	20.32	31.95	16.27	10.22	17.39	27.91	38.54	29.94	42.92	54.81	25.82	17.60	28.96	40.67	50.18	48.65	51.41	52.37	66.06	64.36	66.78	68.74
RE-Net	45.24	37.82	48.53	58.92	43.02	36.26	45.61	56.03	57.66	51.86	60.40	68.60	41.19	34.62	43.96	53.11	52.27	50.92	52.73	53.57	64.68	62.94	65.11	67.82
Our encoder + TuckER	46.42	38.94	50.25	59.80	44.56	37.87	47.46	57.06	59.93	54.59	62.65	69.64	39.66	30.60	44.74	54.23	51.98	50.89	52.47	53.78	63.20	60.54	64.47	67.80
Our encoder + Distmult	46.68	41.20	48.64	57.05	44.00	38.64	45.78	54.27	58.89	54.42	60.76	67.47	41.23	35.19	42.99	52.79	52.49	51.71	52.82	53.68	67.44	66.66	67.46	68.75

Table 3: Extrapolated link prediction results on six datasets. Evaluation metrics are time-unaware filtered MRR (%) and Hits@1/3/10 (%). The best results are marked in bold.

Datasets	ICEWS05-15 - raw				ICEWS05-15 - dep filtered				ICEWS05-15 - indep filtered			
Model	MRR	Hits@1	Hits@3	Hits@10	MRR	Hits@1	Hits@3	Hits@10	MRR	Hits@1	Hits@3	Hits@10
RE-Net	4.96	2.20	5.39	10.12	5.02	2.29	5.49	10.12	5.50	2.95	5.93	10.26
Our encoder + TuckER w.o.jump	5.13	2.58	5.67	9.91	5.18	2.64	5.70	9.94	5.98	3.24	6.71	10.67
Our encoder + Distmult w.o.jump	3.72	2.05	3.80	6.76	3.76	2.09	3.82	6.77	4.09	2.46	4.17	6.99
Our encoder + TuckER	5.74	3.07	6.48	10.74	5.81	3.16	6.52	10.78	6.75	4.11	7.60	11.54
Our encoder + Distmult	5.00	2.70	5.67	9.16	5.05	2.78	5.69	9.17	5.69	3.45	6.27	9.69

Table 4: Inductive extrapolated link prediction results on ICEWS05-15. Evaluation metrics are raw, time-aware filtered, and time-unaware filtered MRR (%), Hits@1/3/10 (%). w.o.jump means without stochastic jump method. The best results are marked in bold.

mation right before the prediction timestamp is likely to be missing. This arouses the interest in evaluating the graph learning models by predicting the links in the farther future. For the above mentioned example, it can be interpreted as predicting the links happening at t' , where $t' > t + 1$, given the same graph information $\mathbb{G} = \{\mathcal{G}(t - k), \dots, \mathcal{G}(t)\}$. Based on this idea, we define a new evaluation task, namely long horizontal link forecasting, and compare the performance achieved by our model with the performance achieved by RE-Net which is also a method designed specifically for extrapolated link forecasting.

To perform long horizontal link forecasting, we adjust the integral length according to how far the future we want to predict. As described in Figure 3, Given k graph snapshots, we can infer the graph hidden state at $t + \Delta t$ by doing the integration with the ODE solver for $k + 1$ times. For the first k steps, e.g. integration from $t - k$ to $t - k + 1$, the integration length corresponds to the unit time between the neighboring timestamps. However, for the last step, i.e. integration from t to $t + \Delta t$, the integration length corresponds to Δt , which may differ according to how far the future we want to predict. The larger Δt is, the longer the length is for the last step of integration. For RE-Net, we first update the entity history until t and then reuse the graph information at t , i.e. $\mathcal{G}(t)$, to update the entity history from t to $t + \Delta t$. The updated history until $t + \Delta t$ is utilized to predict the links at $t + \Delta t$. In this case, both our model and RE-Net only use the graph information at t and before t to predict the future Δt away.

We report the results corresponding to different Δt on ICEWS05-15. From Figure 4 (b), we observe that our model outperforms RE-Net in long horizontal link forecasting. The gap between the performances of the two models diminishes as

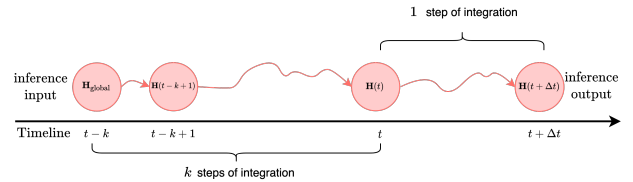


Figure 3: Graphical illustration of long horizontal link forecasting. Given a sequence of graph snapshots $\mathbb{G} = \{\mathcal{G}(t - k), \dots, \mathcal{G}(t)\}$, whose length is k , test quadruples at $t + \Delta t$ are to be predicted.

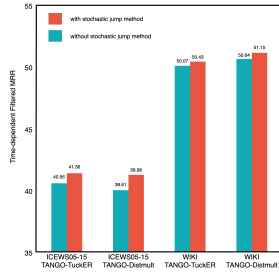
Δt increases. This trend can be explained in the following way. Our model employs an ODE solver to integrate the graph hidden state over time. As Δt increases, the integration length of the last integral, similar to the integration from t to $t + \Delta t$ shown in Figure 3, also grows accordingly. The graph snapshot used inside the neural network F_{model} for this integration is $\mathcal{G}(t)$. As the integration length becomes longer, our model will go through more graph aggregation layers, which at the same time, will make our model more likely to learn more about the structural information provided only by $\mathcal{G}(t)$, thus leading to the degradation in capturing the information regarding the links not appearing in $\mathcal{G}(t)$.

4.2.5 Ablation Study

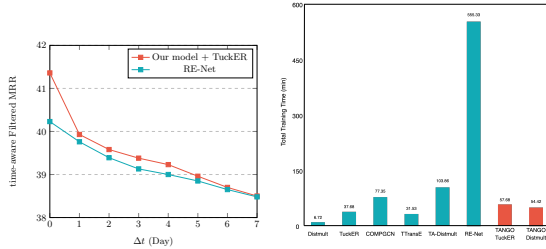
To observe the effectiveness of our stochastic jump method, we conduct an ablation study on two datasets, i.e. ICEWS05-15 and WIKI. We choose these two datasets as the representative of the first type and the second type of datasets. The difference between the two types is explained in Appendix B.1. The improvement of the time-aware filtered MRR brought by the stochastic jump method is illustrated in Figure 4 (a). The stochastic jump method can effectively boost the model performance by incorporating the information provided by the stochastic jump events.

4.2.6 Time Cost Analysis

Keeping the training time short while achieving a strong performance is significant in model evaluation. We report in Figure 4 (c) the total training time of our model as well as



(a) Ablation Study.



(b) Long Horizontal Link Forecasting. (c) Time Cost Analysis.

Figure 4: (a) Time-aware filtered MRR of our model with or without the stochastic jump method on ICEWS05-15 and WIKI. (b) Time-aware filtered MRR on ICEWS05-15 corresponding to different Δt . (c) The training time of baselines and our model on ICEWS14. Columns marked as orange denote the time consumed by our model.

the baselines on ICEWS14. As shown in Figure 4 (c), static KG reasoning methods on average require less training time than temporal methods. Though the total training time for TTransE is also short, its performance is poor as reported in the former sections. TA-DistMult consumes more time than our model and is also beaten by our model in performance. RE-Net is the strongest baseline in performance, however, it requires almost 10 times as much as the total training time of our model. our model ensures a short training time while maintaining the state-of-the-art performance for extrapolated link prediction, which shows the superiority of our model.

5. CONCLUSIONS

We propose a novel model for extrapolated link prediction. It is the first model using NODE in temporal knowledge graph reasoning and it learns a continuous graph representation over time. We couple our model with the stochastic jump method, a method to capture the information provided by the change of knowledge graph facts over time. According to experiment results, our model achieves state-of-the-art performance and beats all the baselines. Besides, We also propose two new tasks to validate the potential of link forecasting models, namely inductive link prediction and long horizontal link forecasting. Our model performs well in both tasks and shows its great potential.

6. REFERENCES

[1] I. Balazevic, C. Allen, and T. Hospedales. TuckER:

Tensor factorization for knowledge graph completion. In *Proceedings of the 2019 Conference on Empirical Methods in Natural Language Processing and the 9th International Joint Conference on Natural Language Processing (EMNLP-IJCNLP)*, pages 5185–5194, Hong Kong, China, Nov. 2019. Association for Computational Linguistics.

- [2] J.-P. Berrut and L. N. Trefethen. Barycentric lagrange interpolation. *SIAM review*, 46(3):501–517, 2004.
- [3] A. Bordes, N. Usunier, A. Garcia-Durán, J. Weston, and O. Yakhnenko. Translating embeddings for modeling multi-relational data. In *Proceedings of the 26th International Conference on Neural Information Processing Systems - Volume 2, NIPS’13*, page 2787–2795, Red Hook, NY, USA, 2013. Curran Associates Inc.
- [4] E. Boschee, J. Lautenschlager, S. O’Brien, S. Shellman, J. Starz, and M. Ward. ICEWS Coded Event Data, 2015.
- [5] R. T. Chen, Y. Rubanova, J. Bettencourt, and D. K. Duvenaud. Neural ordinary differential equations. In *Advances in neural information processing systems*, pages 6571–6583, 2018.
- [6] T. Daulbaev, A. Katrutza, L. Markeeva, J. Gusak, A. Cichocki, and I. Oseledets. Interpolated adjoint method for neural odes. *arXiv preprint arXiv:2003.05271*, 2020.
- [7] M. Defferrard, X. Bresson, and P. Vandergheynst. Convolutional neural networks on graphs with fast localized spectral filtering. In *Advances in neural information processing systems*, pages 3844–3852, 2016.
- [8] S. Deng, H. Rangwala, and Y. Ning. Dynamic knowledge graph based multi-event forecasting. In *Proceedings of the 26th ACM SIGKDD International Conference on Knowledge Discovery & Data Mining*, pages 1585–1595, 2020.
- [9] A. García-Durán, S. Dumančić, and M. Niepert. Learning sequence encoders for temporal knowledge graph completion. In *Proceedings of the 2018 Conference on Empirical Methods in Natural Language Processing*, pages 4816–4821, Brussels, Belgium, Oct.-Nov. 2018. Association for Computational Linguistics.
- [10] J. Gilmer, S. S. Schoenholz, P. F. Riley, O. Vinyals, and G. E. Dahl. Neural message passing for quantum chemistry. *arXiv preprint arXiv:1704.01212*, 2017.
- [11] W. Glover and J. Lygeros. A stochastic hybrid model for air traffic control simulation. In *International Workshop on Hybrid Systems: Computation and Control*, pages 372–386. Springer, 2004.
- [12] R. Goel, S. M. Kazemi, M. Brubaker, and P. Poupart. Diachronic embedding for temporal knowledge graph completion. In *Proceedings of the AAAI Conference on Artificial Intelligence*, volume 34, pages 3988–3995, 2020.

- [13] W. Hamilton, Z. Ying, and J. Leskovec. Inductive representation learning on large graphs. In *Advances in neural information processing systems*, pages 1024–1034, 2017.
- [14] Z. Han, P. Chen, Y. Ma, and V. Tresp. Dyernie: Dynamic evolution of riemannian manifold embeddings for temporal knowledge graph completion. *arXiv preprint arXiv:2011.03984*, 2020.
- [15] Z. Han, Y. Wang, Y. Ma, S. Guünnemann, and V. Tresp. The graph hawkes network for reasoning on temporal knowledge graphs. *arXiv preprint arXiv:2003.13432*, 2020.
- [16] J. P. Hespanha. Stochastic hybrid systems: Application to communication networks. In *International Workshop on Hybrid Systems: Computation and Control*, pages 387–401. Springer, 2004.
- [17] J. Jia and A. R. Benson. Neural jump stochastic differential equations. In *Advances in Neural Information Processing Systems*, pages 9847–9858, 2019.
- [18] W. Jin, H. Jiang, M. Qu, T. Chen, C. Zhang, P. Szekely, and X. Ren. Recurrent event network: Global structure inference over temporal knowledge graph. *arXiv preprint arXiv:1904.05530*, 2019.
- [19] D. P. Kingma and J. Ba. Adam: A method for stochastic optimization, 2017.
- [20] T. N. Kipf and M. Welling. Semi-supervised classification with graph convolutional networks. *arXiv preprint arXiv:1609.02907*, 2016.
- [21] J. Leblay and M. W. Chekol. Deriving validity time in knowledge graph. In *Companion Proceedings of the The Web Conference 2018*, pages 1771–1776, 2018.
- [22] K. Leetaru and P. A. Schrodtt. Gdelt: Global data on events, location, and tone, 1979–2012. Citeseer.
- [23] X. Li, O. Omotere, L. Qian, and E. R. Dougherty. Review of stochastic hybrid systems with applications in biological systems modeling and analysis. *EURASIP Journal on Bioinformatics and Systems Biology*, 2017(1):8, 2017.
- [24] F. Mahdisoltani, J. Biega, and F. M. Suchanek. Yago3: A knowledge base from multilingual wikipedias. 2013.
- [25] G. A. Miller. Wordnet: a lexical database for english. *Communications of the ACM*, 38(11):39–41, 1995.
- [26] M. Niepert, M. Ahmed, and K. Kutzkov. Learning convolutional neural networks for graphs. In *International conference on machine learning*, pages 2014–2023, 2016.
- [27] A. Paszke, S. Gross, F. Massa, A. Lerer, J. Bradbury, G. Chanan, T. Killeen, Z. Lin, N. Gimelshein, L. Antiga, et al. Pytorch: An imperative style, high-performance deep learning library. In *Advances in neural information processing systems*, pages 8026–8037, 2019.
- [28] L. S. Pontryagin. *Mathematical theory of optimal processes*. Routledge, 2018.
- [29] A. Singhal. Introducing the knowledge graph: things, not strings. *Official google blog*, 5, 2012.
- [30] R. Trivedi, H. Dai, Y. Wang, and L. Song. Know-evolve: Deep temporal reasoning for dynamic knowledge graphs, 2017.
- [31] L. R. Tucker. The extension of factor analysis to three-dimensional matrices. 1964.
- [32] E. E. Tyrtysnikov. *A brief introduction to numerical analysis*. Springer Science & Business Media, 2012.
- [33] S. Vashishth, S. Sanyal, V. Nitin, and P. Talukdar. Composition-based multi-relational graph convolutional networks. *arXiv preprint arXiv:1911.03082*, 2019.
- [34] Z. Wu, S. Pan, F. Chen, G. Long, C. Zhang, and S. Y. Philip. A comprehensive survey on graph neural networks. *IEEE Transactions on Neural Networks and Learning Systems*, 2020.
- [35] B. Yang, W.-t. Yih, X. He, J. Gao, and L. Deng. Embedding entities and relations for learning and inference in knowledge bases. *arXiv preprint arXiv:1412.6575*, 2014.

Datasets	ICEWS14 - raw				ICEWS18 - raw				ICEWS05-15 - raw				GDELTA - raw				WIKI - raw				YAGO - raw			
Model	MRR	HITS@1	HITS@3	HITS@10	MRR	HITS@1	HITS@3	HITS@10	MRR	HITS@1	HITS@3	HITS@10	MRR	HITS@1	HITS@3	HITS@10	MRR	HITS@1	HITS@3	HITS@10	MRR	HITS@1	HITS@3	HITS@10
Distmult	10.35	5.25	10.86	20.47	16.10	8.99	17.88	30.49	20.60	12.78	22.86	36.66	12.36	6.45	12.64	23.66	14.37	10.49	16.70	20.77	35.47	27.85	39.70	49.87
TuckER	12.76	6.63	13.45	24.90	19.99	11.70	22.35	36.71	22.93	14.34	25.63	40.28	12.23	6.23	12.44	23.74	14.46	10.57	16.76	20.84	36.12	28.44	40.23	50.84
COMPGCN	12.91	6.73	13.54	25.23	18.94	10.87	20.89	35.38	23.44	14.71	26.07	41.31	12.56	6.51	12.83	24.17	15.10	11.16	17.26	21.64	36.28	28.14	40.32	52.27
TTransE	6.89	1.36	6.60	18.18	7.92	1.75	8.00	21.02	15.36	4.62	18.86	38.14	5.46	0.49	4.92	15.06	19.53	12.34	23.11	32.47	26.18	12.36	36.16	48.00
TA-DistMult	9.92	4.39	9.99	20.90	11.05	5.24	11.72	22.55	24.03	14.37	27.36	44.04	11.00	4.95	11.39	22.45	27.33	19.94	32.05	39.42	45.54	36.54	51.08	62.15
RE-Net	23.84	14.60	26.48	42.58	26.62	16.91	30.26	45.82	39.31	28.88	44.40	59.38	19.17	11.95	20.48	33.26	31.10	25.31	34.13	41.33	46.28	37.52	51.77	61.55
Our encoder + TuckER	24.29	15.02	27.11	43.01	27.31	17.57	31.04	46.43	40.35	29.61	45.87	60.97	19.22	11.97	20.52	33.28	30.87	24.82	34.02	41.35	47.23	38.94	52.68	61.68
Our encoder + Distmult	22.84	14.13	25.33	40.48	25.43	16.19	28.94	43.55	38.99	28.81	44.15	58.41	18.77	11.68	19.97	32.53	31.16	25.35	34.15	41.17	48.70	40.17	54.82	63.04

Table 5: Extrapolated link prediction results on GDELTA, WIKI and YAGO. Evaluation metrics are raw MRR (%) and Hits@1/3/10 (%). The best results are marked in bold.

APPENDIX

A. ALGORITHM OF INFERENCE PROCEDURE

Algorithm 1: Temporal Graph Representation Inference

Input: Global graph embedding $\mathbf{H}_{\text{global}}$, timestamps $t - k, \dots, t$, tKG snapshots $\mathcal{G}(t - k), \dots, \mathcal{G}(t)$, adjacency matrices $\mathbf{T}(t - k), \dots, \mathbf{T}(t)$, neural network F_{model} , jump coefficient w .

Output: Graph hidden state $\mathbf{H}(t + 1)$ at $t + 1$.

```

1 def set_graph( $F_{\text{model}}, \mathcal{G}(t_0)$ ):
2   for every graph aggregation layer  $l$  in  $F_{\text{model}}$  do
3      $\mathcal{G}^l = \mathcal{G}(t_0)$ 
4     Input  $\mathcal{G}^l$  into  $F_{\text{model}}$ 
5   return  $F_{\text{model}}$ 
6 def set_jump( $F_{\text{model}}, \mathbf{T}(t_0), \mathbf{T}(t_0 + 1)$ ):
7    $\mathbf{T}^\Delta(t_0) = \mathbf{T}(t_0 + 1) - \mathbf{T}(t_0)$ 
8    $\mathbf{T}^\Delta = \mathbf{T}^\Delta(t_0)$ 
9   Input  $\mathbf{T}^\Delta$  into  $F_{\text{model}}$ 
10  return  $F_{\text{model}}$ 
11 Initialize  $\mathbf{H}(t - k) = \mathbf{H}_{\text{global}}$ .
12 for  $t'$  in  $[t - k, t]$  do
13    $F_{\text{model}} = \text{set\_graph}(F_{\text{model}}, \mathcal{G}(t'))$ 
14   if  $t' = t$  then
15      $F_{\text{model}} = \text{set\_jump}(F_{\text{model}}, \mathbf{T}(t'), \mathbf{T}(t' + 1))$ 
16   else
17      $F_{\text{model}} = \text{set\_jump}(F_{\text{model}}, \mathbf{T}(t - 1), \mathbf{T}(t))$ 
18    $\mathbf{H}(t' + 1) = \text{ODESolve}(\mathbf{H}(t'), F_{\text{model}}, t', t' + 1, \Theta_{\text{model}}, w)$ 

```

Algorithm 1 describes the inference procedure of our model. `set_graph` and `set_jump` are defined as same in Figure 2. They stand for two functions to input graph snapshots and jump tensors into neural network F_{model} . In line 3, \mathcal{G}^l denotes the input graph of the l^{th} aggregation layer in F_{model} , and in line 7, \mathbf{T}^Δ denotes the input jump tensor of F_{model} .

B. EXPERIMENT DETAILS

Dataset	N_{train}	N_{valid}	N_{test}	$ \mathcal{V} $	N_{rel}	Time Granularity
ICEWS14 [30]	323,895	–	341,409	12,498	260	24 hours
ICEWS18 [4]	373,018	45,995	49,545	23,033	256	24 hours
ICEWS05-15 [9]	369,104	46,188	46,037	10,488	251	24 hours
GDELTA [22]	1,734,399	238,765	305,241	7,691	240	15 mins
WIKI [21]	539,286	67,538	63,110	12,554	24	1 year
YAGO [24]	161,540	19,523	20,026	10,623	10	1 year

Table 6: Dataset statistics.

B.1 Dataset Details

The details of the datasets are stated in Table 6. As explained in [18], the difference between the first type (ICEWS datasets and GDELTA) and the second type (WIKI and YAGO) of tKG datasets is that the first type datasets consist of facts

that happen multiple times (even periodically) in the whole timeline, while the facts from the second type datasets last much longer and are not likely to happen multiple times. In all the datasets, a fact spans across several timestamps is transformed, following the fashion of [18], into several separate events that take place on a consecutive sequence of timestamps. For example, a fact (s, r, o) which lasts from t_s to t_e is transformed into several events $\{(s, r, o, t_s), (s, r, o, t_s + 1_t), \dots, (s, r, o, t_e)\}$, where 1_t represents a unit time.

B.2 Time aware Filtered Setting Example

The following example is stated to explain the reason why the time-aware filtered results are fairer than the time-unaware filtered results. For example, in ICEWS14, we have a test quadruple of interest (Xi Jinping, Make a visit, New Zealand, 2014-11-26) in the test set, and we want to perform the link prediction on the object prediction query (Xi Jinping, Make a visit, ?, 2014-11-26). We also have another quadruple (Xi Jinping, Make a visit, South Korea, 2014-07-05) in the test set. According to the time-unaware filtered setting [3], (Xi Jinping, Make a visit, South Korea) will be taken as the corrupted triplet, thus causing the triplet (Xi Jinping, Make a visit, South Korea) filtered. However, it is unreasonable, because (Xi Jinping, Make a visit, South Korea) is not valid at 2014-11-26. We, therefore, use the time-aware filtered setting, which, in our example, will only filter the triplets (Xi Jinping, Make a visit, o) appearing at 2014-11-26. Here, o denotes all the objects which form triplets with Xi Jinping and Make a visit at timestamp 2014-11-26.

B.3 Detailed Experimental Settings of Base lines

We implement Distmult by ourselves. The embedding sizes are 200. We use the binary cross-entropy loss for parameter learning.

We use the original implementation of TuckER¹. The embedding sizes are 200. We use the binary-cross entropy loss for parameter learning.

We use the original implementation of COMPGCN². We choose COMPGCN coupled with multiplication operator and Distmult score function. The embedding sizes are 200. The hidden layer size is 150. We use the binary cross-entropy loss for parameter learning.

We use the implementation of TTransE and TA-Distmult provided in [18]³. The embedding sizes are 200. We use the binary cross-entropy loss for parameter learning. For TA-Distmult, the vocabulary of temporal tokens consists of year, month, day for all the datasets except GDELTA. On GDELTA, the vocabulary consists of year, month, day, hour,

¹<https://github.com/ibalazevic/TuckER>

²<https://github.com/mallabiisc/CompGCN>

³<https://github.com/INK-USC/RE-Net>

minute.

We use the original implementation of RE-Net⁴. The embedding sizes are 200. We follow the setting proposed in [18]. We set the history length to 10 and use the max-pooling when training the global model. In testing, we use the ground truth graph information for link prediction, rather than performing multi-step inference.

All the baselines are trained with Adam Optimizer [19] and the batch size is set to 512.

B.4 Raw Results

Raw results are stated in Table 5. our model outperforms all the baseline methods.

B.5 Inductive Link Prediction Example

In a tKG dataset, there exist a group of entities that have interactions with other entities only in the test set. For example, in the test set of ICEWS05-15, we have a test quadruple (Raheel Sharif, Express intent to meet or negotiate, Chaudhry Nisar Ali Khan, 2014-12-29). The entity Raheel Sharif does not appear in the training set, indicating that the aforementioned quadruple contains an entity that only has interactions with other entities in the test set. We call the evaluation of this kind of test quadruples the inductive link prediction analysis because it analyzes the performance of the model regarding the entities which are not seen in the training process.

⁴<https://github.com/INK-USC/RE-Net>